Deciphering myeloid (progenitor) cell function and communication in (tumor) tissues

Lei, X.

Chapter 6

Flagellin/TLR5 stimulate myeloid progenitors to enter lung tissue and to locally differentiate into macrophages

Xin Lei[1,2#], Jara Palomero[2#], Iris de Rink[3], Tom de Wit[1,2], Martijn van Baalen[4], Yanling Xiao[1,2*], Jannie Borst[1,2*]

[1]Division of Tumor Biology and Immunology, The Netherlands Cancer Institute, Amsterdam The Netherlands; [2]Department of Immunology and Oncode Institute, Leiden University Medical Center, The Netherlands; [3]Genomics Facility, The Netherlands Cancer Institute, Amsterdam, The Netherlands; [4]Flow Cytometry Facility, The Netherlands Cancer Institute, Amsterdam, The Netherlands

[*]Corresponding authors
[#]These authors contributed equally

Front. Immunol., 2021; 12: 621665.
DOI: 10.3389/fimmu.2021.621665

Abstract

Toll-like receptor 5 (TLR5) is the receptor of bacterial Flagellin. Reportedly, TLR5 engagement helps to combat infections, especially at mucosal sites, by evoking responses from epithelial cells and immune cells. Here we report that TLR5 is expressed on a previously defined bipotent progenitor of macrophages (MΦ) and osteoclasts (OC) that resides in the mouse bone marrow (BM) and circulates at low frequency in the blood. *In vitro*, Flagellin promoted the generation of MΦ, but not OC from this progenitor. *In vivo*, intranasal Flagellin inoculation induced recruitment of intravenously transferred MΦ / OC progenitors into the lung and their rapid, local differentiation into MΦ. Recruitment of the MΦ /OC progenitors from the blood stream into the lung was likely promoted by the CCL2/CCR2 axis, since the progenitors expressed CCR2 and type 2 alveolar epithelial cells (AEC) produced CCL2 upon stimulation by Flagellin. Moreover, CCR2 blockade reduced migration of the MΦ/OC progenitors towards lung exudate from Flagellin-inoculated mice. Our study reveals a novel role of the Flagellin/TLR5 axis in recruiting circulating MΦ/OC progenitors into infected tissue and stimulating these progenitors to locally differentiate into MΦ. The progenitor pathway to produce MΦ may act, next to monocyte recruitment, to fortify host protection against bacterial infection at mucosal sites.

Key words

Flagellin, TLR5, Myelopoiesis, macrophage, Epithelium, CCR2

Introduction

Epithelial cells are the first line of defense against infection[1, 2]. Tissue resident myeloid cells contribute to defense once epithelial integrity is broken. At steady state, peripheral tissues harbor resident MΦ that have an embryonic origin and migratory dendritic cells (DC) that are constantly generated from hematopoietic progenitors in the BM[3, 4]. Upon infection or tissue damage, neutrophils and monocytes are recruited from the blood into peripheral tissues[5]. All myeloid cell types have pattern recognition receptors (PRRs), such as toll-like receptors (TLR) that allow them to recognize and respond to pathogen-associated molecular patterns (PAMP) and self-derived damage-associated molecular patterns (DAMPs)[6].

TLR5 recognizes Flagellin, the primary structural component of bacterial flagella that is a major trigger of innate immunity[7, 8], particularly at mucosal sites[9, 10]. TLR5 is located at the basal side of epithelia and thereby senses the invasion of potentially pathogenic bacteria, such as Salmonella[11, 12]. In epithelial cells, Flagellin induces expression of proinflammatory cytokines, chemokines and nitric oxide[13]. Myeloid cell types as well as T cells also respond to Flagellin[10, 14, 15]. In the mouse intestine, TLR5 on $CD11c^+$ cells in the lamina propria proved to be essential for the defense against pathogenic bacteria[16]. Flagellin is a key antigen in human Crohn's disease[17], supporting its role in evoking both innate and adaptive immunity. Accordingly, many studies address the potency of Flagellin as a vaccine adjuvant[18].

TLRs are also found on different hematopoietic stem and progenitor cells (HSPC), including hematopoietic stem cells (HSC), common myeloid progenitors (CMP), and granulocyte (G)/MΦ progenitors (GMP). TLR signaling preferentially stimulates myeloid development from HSPC in the absence of homeostatic cytokines. This suggests a role for TLR signaling in innate immune cell replenishment[19–21]. Recently, it has been reported that systemic Flagellin administration drives rapid TLR5-dependent HSC cell proliferation and a great increase in multipotent progenitors. Neutrophils produced by these progenitors protected mice against total body irradiation[22]. The generation of myeloid cells from hematopoietic progenitors fits in the concept of "emergency hematopoiesis." Herein, myeloid cells are generated de novo from progenitors, to boost immune defense and tissue repair[23].

OC are also part of the myeloid lineage[24–26] and play a role in hematopoiesis by creating niches for stem cells in the BM[27]. OCs and osteoblasts maintain bone homeostasis via bidirectional communication. This process is deregulated during

chronic inflammation, such as in rheumatoid arthritis, leading to bone remodeling[28, 29]. We previously found that the GMP as found in mouse and human BM can also give rise to OCs and DC. We thus redefined the GMP as oligopotent G/ MΦ/OC/DC progenitor (GMODP). In addition, we found that the GMODP stepwise gives rise to a more committed MΦ/OC/DC progenitor (MODP) and a bipotent M8/OC progenitor (MOP)[25, 26]. We here report that TLR5 cell surface expression progressively increases with MΦ/OC commitment in this hierarchy and that Flagellin/TLR5 promotes MΦ- but not OC differentiation from MOP. Furthermore, our study supports a scenario wherein TLR5 on bipotent MΦ/OC myeloid progenitors helps replenish MΦ for protection against bacterial infection at mucosal sites.

Results

TLR5 is differentially expressed between MODP and MOP

In a previous study, we have redefined the human GMP as oligopotent progenitor of G, MΦ, OC, and DC and termed it GMODP. Downstream of it, we identified a more committed oligopotent progenitor of MΦ, OC, and DC (MODP)[25] (Fig. 1A). In the mouse, we identified common progenitors of MΦ, OC, and DC in a $B220^{-}CD11b^{low/-}$c-Kit^{+}c-Fms^{+} BM cell population (Fig. 1B). This population could be dissected into a $CD27^{high}$ MODP and a downstream $CD27^{low/-}$ MΦ/OC progenitor (MOP)[26] (Fig. 1A, C). We analyzed in one staining procedure the cell surface phenotypes of MODP and MOP populations and the main hematopoietic progenitor populations HSC, multipotent progenitor (MPP), common lymphoid progenitor (CLP), CMP, and GMP, as defined by Weissman and Shizuru[30]. This analysis shows that the MODP and MOP populations are distinct from their upstream progenitors, including the GMP (Fig. S1A–C). The developmental relationship between MODP and MOP was further validated by mRNA deep sequencing[26]. Among transcripts that discriminated between MODP and MOP were *Cd27* (*Tnfrsf7*), but also *Tlr5* (Fig. 1D). TLR5 was also differentially expressed between the two progenitor cell populations at the protein level, as determined by flow cytometry. The cell surface expression of TLR5 was significantly higher on MOP than on MODP cells that occur in low frequency.

TLR5 cell surface level correlates with MOP commitment to MΦ/OC differentiation

Given that TLR5 cell surface levels on the MOP population were heterogeneous and higher than on the MODP population, we examined whether they correlated with commitment to MΦ and OC differentiation (Fig. 2A). For this purpose, $TLR5^{low/-}$ and $TLR5^{high}$ MOP cell subsets were purified from BM cells by flow cytometry-based sorting and in vitro differentiation cultures were performed. To determine differentiation into MΦ, defined as $MHCII^{+}CD11b^{+}F4/80^{+}$ cells (Fig. 2B), progenitor populations were cultured at 2,000 cells per well with M-CSF and analyzed by flow cytometry at successive days until day 6. $TLR5^{low/-}$ and $TLR5^{high}$ MOP-derived cultures had comparable frequencies of MΦ, throughout the entire duration of the culture (Fig. 2C). However, the MΦ yield in absolute cell numbers was higher in the $TLR5^{low/-}$ MOP-derived cultures than in TLR5high MOP-derived cultures (Fig. 2D). This suggests that TLR5high MOP are more committed and less proliferative, as also appeared from microscopic examination (Fig. 2E). In agreement with the notion that TLR5 expression levels correlated with MΦ commitment, TLR5 expression was higher on $MHCII^{+}CD11b^{+}F4/80^{+}$ MΦ than on immature $MHCII^{+}CD11b^{low/-}F4/80^{-}$ cells in a progenitor-derived MΦ differentiation culture (Fig. S2C,D).

To determine differentiation into OC, $TLR5^{low/-}$ and $TLR5^{high}$ MOP were cultured at 2,000 cells per well with RANKL and M-CSF. At day 3 of culture, RANK was expressed on a large part of the cells in both cultures (Fig. 2F). OC are characterized by expression of TRAP and during maturation, single cells fuse to form multinucleated OC of different sizes[31]. At day 6 of culture, OC formation was diagnosed microscopically and quantified by TRAP staining. $TLR5^{high}$ MOP-derived OC had the most mature phenotype, with giant multinucleated $TRAP^{+}$ cells that were not seen in $TLR5^{low/-}$ MOP-derived offspring (Fig. 2G,H), indicating that $TLR5^{high}$ MOP are more committed to OC differentiation than $TLR5^{low/-}$ MOP. Overall, we conclude that cell surface TLR5 levels on the MOP population positively correlate with commitment to MΦ/OC differentiation.

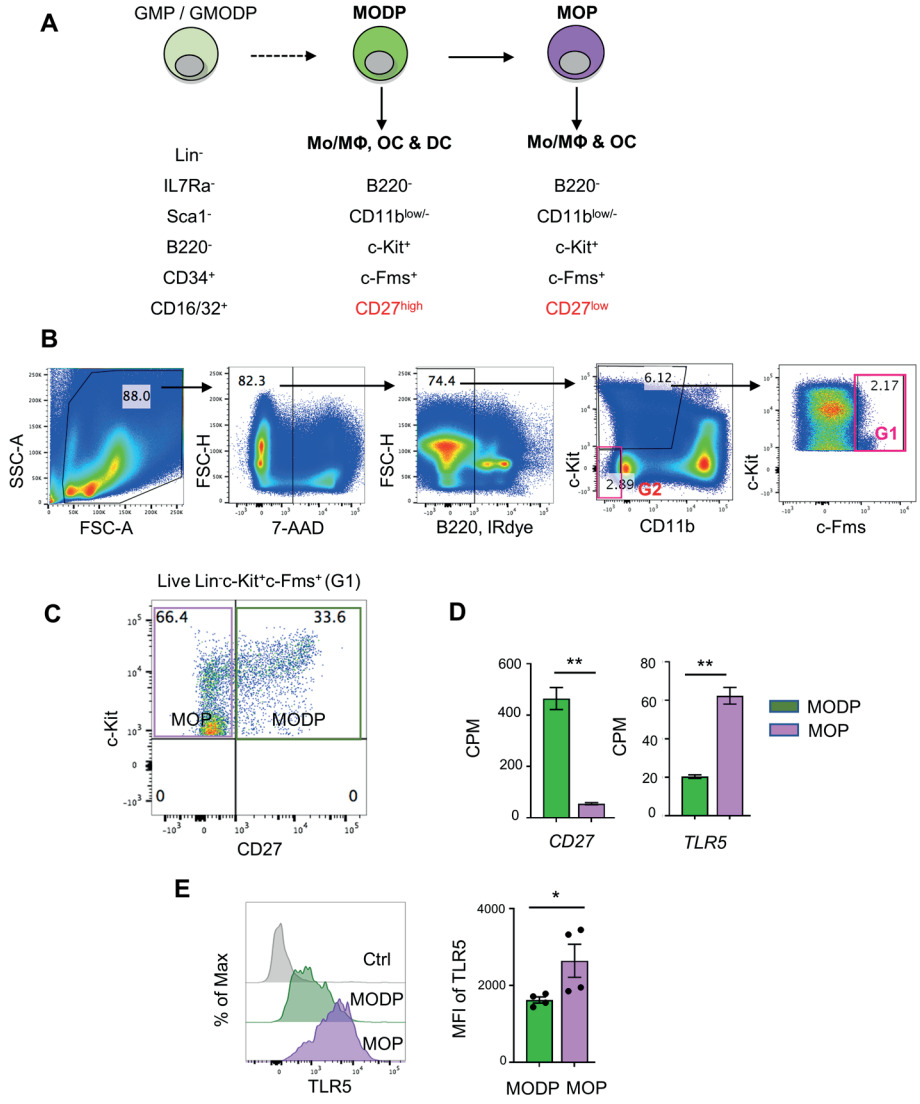

Fig. 1 TLR5 is differentially expressed at transcript and protein levels between MODP and MOP. (**A**) Proposed developmental relationship between GMP/GMODP, MODP, and MOP in murine hematopoiesis and the identifying cell surface markers[24,26]. (**B**) Representative flow cytometry plots depicting gating strategy for B220^{-}CD11b$^{low/-}$c-Kit^{+}c-Fms^{+} BM cells. (**C**) Representative flow cytometry plot depicting how CD27 cell surface expression discriminates MODP and MOP within the B220^{-}CD11b$^{low/-}$c-Kit^{+}c-Fms^{+} BM cell population. (**D**) Data from an earlier study in which BM-derived MODP and MOP were analyzed by RNAseq (GSE97380). Cd27 and Tlr5 mRNA levels depicted are based on normalized read counts (counts per million, CPM) (n = 3, cells pooled from 2 mice per sample)[26]. (**E**) Flow cytometric analysis of TLR5 cell surface expression on MODP and MOP populations. TLR5 FMO was used as control, MFI = median fluorescence intensity. Data are pooled from 2 independent experiments, each with cells from 2 mice. Error bars indicate standard error of the mean (SEM) and unpaired two tailed Student's t-test was used for statistical evaluation (*$p < 0.05$, **$p < 0.01$).

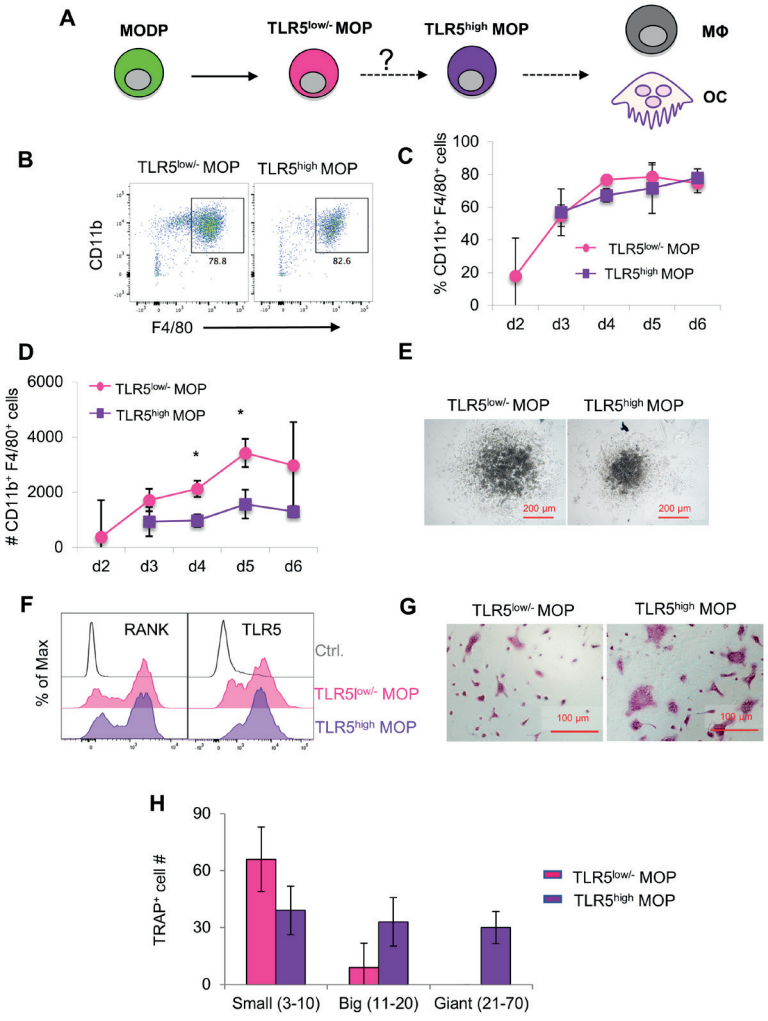

Fig. 2 MΦ and OC differentiation potential of TLR5$^{low/-}$ MOP and TLR5^{high} MOP. (**A**) Proposed developmental path from MOP to MΦ and OC. (**B–H**) M8 and OC differentiation cultures. TLR5$^{low/-}$ and TLR5^{high} MOP were flow cytometrically sorted from pooled BM cells of 3–5 mice, plated at 2,000 cells/well and cultured under MΦ- (M-CSF) (**B–E**) or OC (M-CSF + RANKL) (**F–H**) differentiation conditions. (**B**) Representative flow cytometry plots identifying MΦ as MHCII^{+}CD11b^{+}F4/80^{+} cells in MΦ differentiation cultures at day 5. (**C,D**) Frequencies (%) (**C**) and absolute numbers (#) (**D**) of MHCII^{+}CD11b^{+}F4/80^{+} cells in MΦ differentiation cultures as determined by flow cytometry at days 2–6. Data are pooled from three independent experiments with technical duplicate samples. (**E**) Representative microscopic images of the M8 differentiation cultures at day 5. (**F**) Representative RANK and TLR5 cell surface expression on cells in OC differentiation cultures at day 3. FMO controls were used for RANK and TLR5 staining. (**G**) Representative light microscopic images depicting TRAP-stained cells in OC differentiation cultures at day 6. (**H**) Absolute numbers of TRAP^{+} cells (OC) in OC differentiation cultures at day 6. Cells with multiple nuclei were counted as individual cell and discriminated into small (1–10 nuclei), big (11–20 nuclei) and giant OCs (≥21 nuclei). Data are pooled from two independent experiments, each with technical triplicate samples. Error bars indicate SEM and unpaired two tailed Student's t-test was used for statistical evaluation (*$p < 0.05$).

Flagellin promotes MΦ differentiation from MODP and MOP in vitro

Next, we investigated whether TLR5 signals impacted MΦ - and/or OC differentiation from MODP and MOP. For this purpose, we added Flagellin to the differentiation cultures (Fig. 3A). In presence of M-CSF, both MODP and MOP cells differentiated into MΦ (Fig. 3B). Within 1 day of differentiation, already 30–40% of MOP offspring cells had the MHCII^{+}CD11b^{+}F4/80^{+} MΦ phenotype (Fig. S3A,B), which increased to 50-60% at day 3 (Fig. 3B, lower panel). Addition of Flagellin to M-CSF increased the frequency of MΦ both in MODP- and MOP-derived cultures, as compared to culture with M-CSF alone (Fig. 3B,C). Flagellin alone could also induce MΦ differentiation from the progenitors (Fig. 3B,C). However, live cell yield was significantly lower when Flagellin was present, either alone or in combination with M-CSF (Fig. 3C). To confirm that Flagellin was driving MΦ differentiation via TLR5, we performed MΦ differentiation cultures with BM cells from *Tlr5*$^{+/+}$ and *Tlr5*$^{-/-}$ littermate mice. Cell surface staining validated TLR5 expression on *Tlr5*$^{+/+}$ Lin^{-}c-Kit^{+}c-Fms^{+} BM cells and lack of it on the same cell population from *Tlr5*$^{-/-}$ mice (Fig. S4A,B). In *Tlr5*$^{+/+}$ BM cell cultures the percentage of MΦ increased upon stimulation with M-CSF or Flagellin as compared to the untreated control sample. In contrast, in *Tlr5*$^{-/-}$ BM cell cultures the percentage of MΦ increased only upon stimulation with M-CSF but not Flagellin (Fig. S4C–E). These results indicate that direct sensing of Flagellin by TLR5 on the progenitors promoted their differentiation into MΦ.

To test the impact of Flagellin on OC differentiation, progenitors were cultured with RANKL and M-CSF and offspring cells were sampled at day 6 of culture. Both MODP and MOP differentiated into OC, defined as multinucleated TRAP^{+} cells (Fig. 3D), as previously described[26]. Additional presence of Flagellin did not affect number and maturity of OC offspring from MODP or MOP, as diagnosed by microscopy and TRAP^{+} cell quantification (Fig. 3E). In summary, we found that *in vitro*, TLR5 engagement on MODP and MOP by Flagellin promotes MΦ differentiation, but does not influence OC differentiation.

Flagellin promotes recruitment of MOP into lung tissue and their local differentiation into MΦ

Since Flagellin promoted MΦ differentiation from MODP and MOP *in vitro*, we hypothesized that Flagellin could also promote MΦ differentiation from myeloid progenitors *in vivo*. To test this, we used a mouse model of intranasal (i.n.) inoculation of Flagellin that reportedly prompts a MΦ response in the lung[32]. CD45.1$^+$ MOP were transferred intravenously (i.v.) via the retro-orbital plexus into CD45.2 recipient mice (Fig. 4A; Fig. S5). Flow cytometric settings for detection of CD45.1$^+$ cells in lung, blood and BM of CD45.2 recipient mice were determined prior to adoptive cell transfer (Fig. S6A,B). Furthermore, we verified that flow-sorted CD45.1$^+$ donor MOP were able to differentiate into OC and MΦ *in vitro*, prior to adoptive transfer (Fig. S6C).

We had two groups of CD45.2 mice that both received CD45.1$^+$ MOP and were stimulated 1 day later i.n. with either Flagellin or PBS. After 24 h, cells were isolated from lung, blood and BM of these mice and analyzed by flow cytometry (Fig. 4A, Fig. 5). Strikingly, the frequency and total number of CD45.1$^+$ donor cells were increased upon Flagellin stimulation in the lung, but not in blood or BM (Fig. 4B–D). Likewise the frequency and total number of CD45.1$^+$ MΦ were increased upon Flagellin stimulation in the lung, but not in blood or BM (Fig. 4E–G; Fig. S6D,E,G,H). We also looked at the endogenous response to Flagellin. Frequency and total number of CD45.1$^-$ recipient MΦ (Fig. 4H–J; Fig. S6F,I) increased upon Flagellin stimulation in the lung, but not in blood or BM. We also detected an increase in CD45.1$^-$ recipient MOP in the lung after Flagellin stimulation (Fig. S7A,B). These results suggest that i.n. Flagellin administration recruitment of MOP from the blood circulation into the lung and their local differentiation into MΦ.

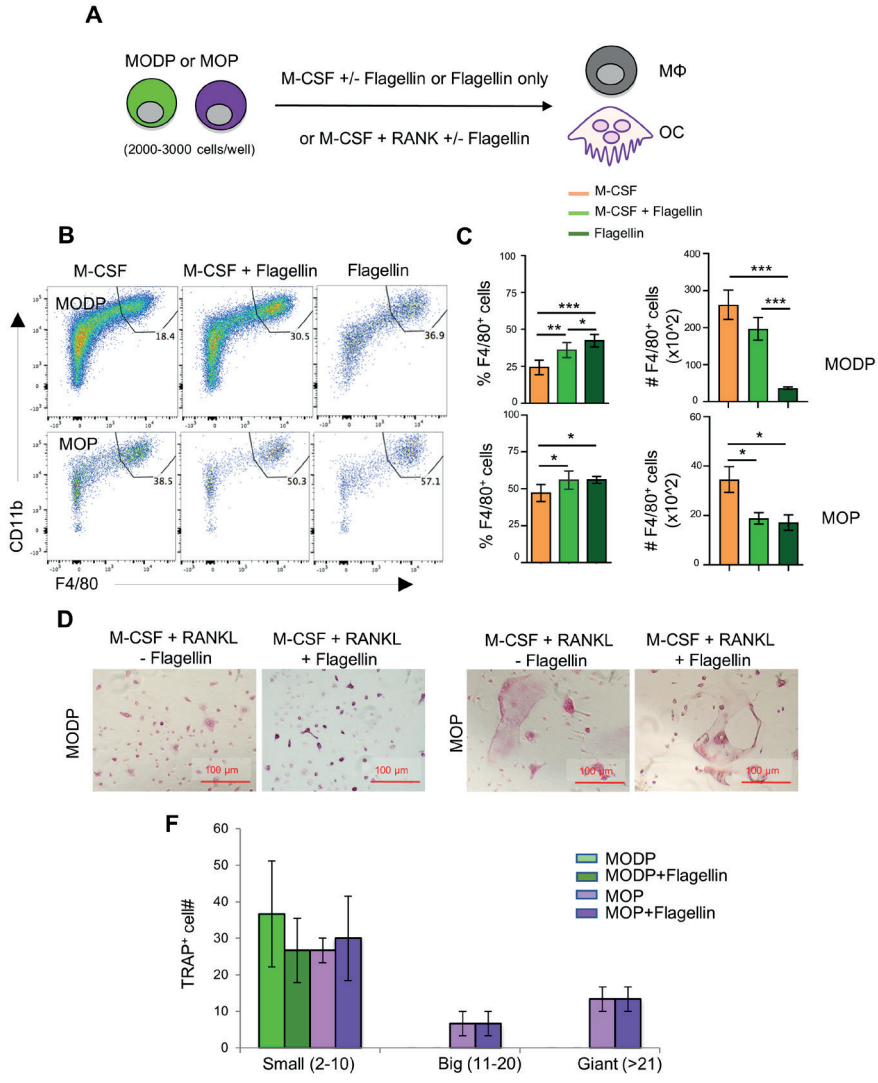

Fig. 3 Flagellin promotes MΦ and OC differentiation from progenitors in vitro. (**A**) Schematic representation of the differentiation cultures. MODP and MOP were flow cytometrically sorted from pooled BM cells of 3–5 mice, plated at 2,000 cells/well and cultured under MΦ- (M-CSF; B,C) or OC differentiation conditions (M-CSF + RANKL; D,E) with or without Flagellin. (**B**) Representative flow cytometry plots depicting the frequencies (%) of MΦ, defined as $MHCII^{+}CD11b^{+}F4/80^{+}$ cells in MΦ differentiation cultures at day 3. (**C**) Quantification of MΦ frequencies and total MΦ cell numbers in the MΦ differentiation cultures. Data are pooled from three independent experiments, each with technical duplicate samples. (**D**) Representative light microscopic images of cells in OC differentiation cultures. (**E**) Quantitative analysis of OC offspring from progenitors under indicated conditions. OC yield was quantified as outlined in the legend of Fig. 2H. Data are pooled from two independent experiments, each with technical duplicate samples. Error bars indicate SEM and one way ANOVA test and Tukey's multiple comparison test were used for statistical evaluation (*p < 0.05, **p < 0.01, ***p < 0.001).

MOP recruitment into lung tissue upon flagellin administration relies on the CCL2-CCR2 axis

We next investigated by which chemokines the adoptively transferred MOP cells might be recruited from the blood into the lung upon i.n. Flagellin administration. For monocyte recruitment from blood into tissue, the CCL2-CCR2 axis is very important [5]. We focused on this possibility, since our transcriptomic (Fig. S8A) and flow cytometric (Fig. S8B, Fig. 5A) data showed that CCR2, the receptor for CCL2, is expressed on MOP, and at a higher level than on MODP. Moreover, alveolar epithelial cells (AEC) reportedly make CCL2 at steady state and increase CCL2 production in response to Flagellin or other stimuli[33–35]. We identified type 2 AEC by flow cytometry in a lung digest, on basis of a $CD45^{-}MHCII^{+}CD31^{-}$ phenotype[36] (Fig. S8C,E). These AEC expressed TLR5 (Fig. S8D) and upregulated CCL2 expression upon stimulation with Flagellin *in vitro* (Fig. 5B,C, Fig. S8E,F) and *in vivo* (Fig. S8G,H). Also, CCR2 was upregulated on MOP in the lung after i.n. Flagellin inoculation (Fig. S7C).

To investigate whether in our in vivo setting, CCL2 from Flagellin-treated airway cells may be involved in attracting $CCR2^{+}$ MOP (or MODP) into the lung, we performed *in vitro* transwell assays. LLF from mice (see Methods) was placed in the lower chambers of a transwell plate and total BM cells or flow sorted MOP were plated in the upper chambers (Fig. 5D). After 12 h, the MODP or MOP in the lower chambers were flow cytometrically determined and quantified (Fig. S9). In the experiments with total BM cells as input (Fig. 5E), both MODP and MOP migrated more efficiently toward LLF from mice that had received Flagellin as compared to PBS, with the MOP being most efficient (Fig. 5E). This was confirmed for MOP, in experiments with purified MOP as input (Fig. 5F). Importantly, in these experiments, CCR2 blockade with specific antibody added to the upper chambers inhibited the migration of MOP toward LLF from Flagellin-treated mice, but not from PBS-treated mice (Fig. 5F). Our collective data suggest that MOP migrate into the lung upon i.n. Flagellin stimulation by virtue of the CCL2- CCR2 axis (Fig. 5G).

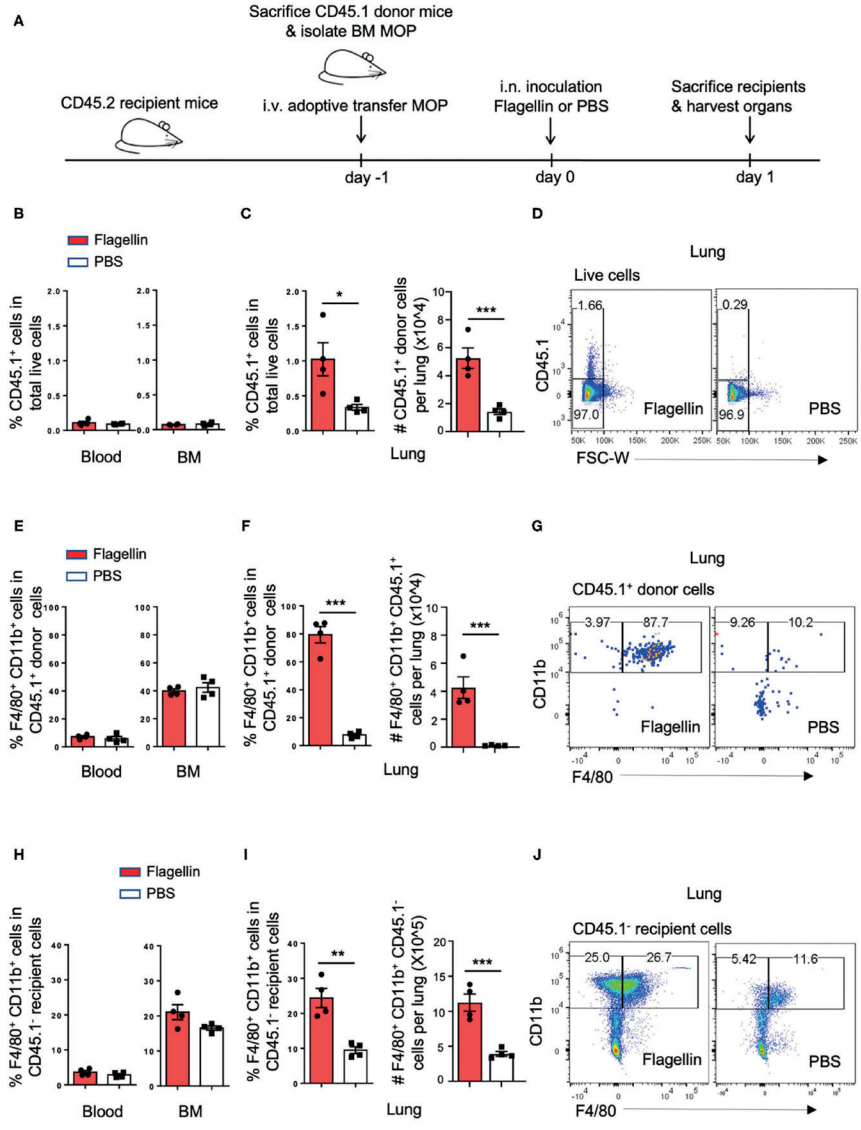

Fig. 4 I.n. Flagellin inoculation promotes MΦ differentiation from MOP in the lung. (**A**) Schematic representation of work flow: MOP were flow cytometrically sorted from pooled BM cells of CD45.1 donor mice (n = 5) and transferred i.v. into CD45.2 recipient mice (n = 8). At 24 h after adoptive cell transfer, 1 µg Flagellin in 50 µl PBS or 50 µl PBS only was inoculated i.n. into the recipient mice (n = 4 for each group) and 24 h later, lung, blood and BM were harvested and dissociated into single cells for flow cytometric analysis. (**B,E,H**) Quantification of $CD45.1^+$ cells, $CD45.1^+$ MOP-derived MΦ and $CD45.1^-$ endogenous MΦ in the blood and BM, respectively, as indicated by frequencies (%). (**C,F,I**) Quantification of $CD45.1^+$ cells, $CD45.1^+$ MOP-derived MΦ and $CD45.1^-$ endogenous MΦ in the lung, as indicated by frequencies (%) and absolute numbers (#). (**D,G,J**) Representative flow cytometric plots depicting adoptively transferred $CD45.1^+$ cells, $CD45.1^+$ MOP-derived MΦ and $CD45.1^-$ endogenous MΦ in the lung, respectively. MΦ were defined as $MHCII^+CD11b^+F4/80^+$ cells. Data are representative of two independent experiments. Error bars indicate SEM, and unpaired two tailed Student's t-test was used for statistical evaluation (*$p < 0.05$, **$p < 0.01$, ***$p < 0.001$).

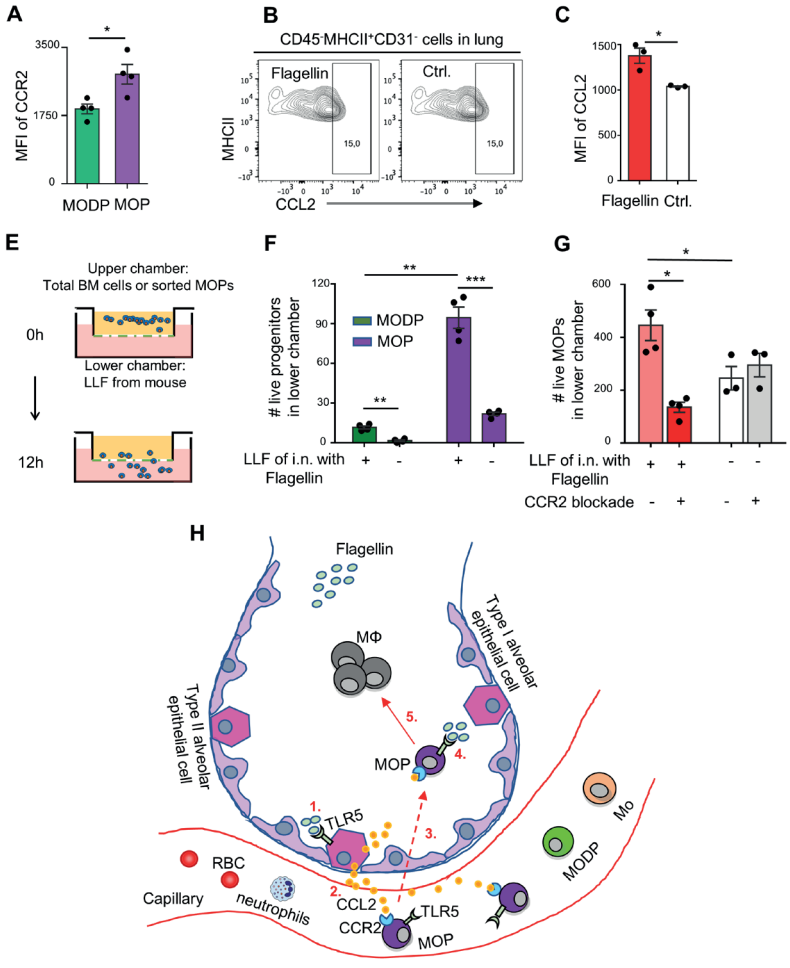

Fig. 5 The CCL2-CCR2 axis promotes Flagellin-induced MOP migration into the lung. (**A**) CCR2 cell surface expression on MODP and MOP from BM (n = 4), as analyzed by flow cytometry (MFI, median fluorescence intensity). Data are representative of two independent experiments. (**B,C**) CCL2 expression in type 2 AEC, defined as $CD45^{-}MHCII^{+}CD31^{-}$ cells, as determined by intracellular staining and flow cytometry in single-cell suspensions of lung tissue after overnight culture in medium with Flagellin or without (Ctrl.). (**B**) Representative flow cytometry plots depicting the frequencies (%) of $CCL2^{+}$ cells within type 2 AEC. CCL2 FMO was used as control. (C) Representative quantitative data from one out of two independent experiments with pooled cells from 3 mice analyzed in technical triplicates. (**D–F**) Transwell migration assay with LLF. (**D**) Experimental set-up. Total BM cells (100,000 cells pooled from three mice) (E), or sorted MOPs (5,000 cells pooled from three mice) (**F**) were added per upper well of a 24 well or 96 well plate and allowed to migrate toward LLF from the two groups of mice (n = 3 4 each) for 12 h under the indicated conditions. Next, cells in the lower chambers were collected and absolute live cell numbers (#) of MODP and MOP (**E**) or MOP (**F**) were determined by flow cytometry. Data are representative of two independent experiments. Error bars indicate SEM, and unpaired two tailed Student's t-test was used for statistical evaluation (*$p < 0.05$, **$p < 0.01$, ***$p < 0.001$). (**G**) Visual representation of the proposed model. Upon i.n. challenge with Flagellin (1), type 2 AEC secrete CCL2 (2) which attracts circulating $CCR2^{+}$ MOP into the lung (3). Subsequently, TLR5 ligation on locally recruited MOP by Flagellin (4) promotes MΦ generation from these progenitors (5). Dashed line indicates speculative part of the model.

Discussion

When a pathogen enters a tissue, epithelial and hematopoietic cells may be activated by PRR and produce chemokines and cytokines that attract immune cells from blood into tissue[5, 37]. In addition, myeloid progenitor cells in the BM may be stimulated to produce monocytes and granulocytes, a process called "emergency myelopoiesis." In this way, myeloid effector cells that are non-dividing and have a short life span can be replenished[37]. The discovery that HSPC can express PRR led to two potential mechanisms for emergency myelopoiesis. One possibility is that upon infection serum levels of cytokines such as GM-CSF, G-CSF, and IL-3 increase, which can promote myelopoiesis from progenitors. Alternatively or in addition, myeloid progenitors may respond directly to the pathogen via PRR and give more offspring. PAMP or serum cytokines do not need enter the BM to reach HSPC, since these cells circulate between blood and BM at steady state[38]. Our study supports a scenario in which bacterial infection at mucosal sites leads to the attraction of myeloid progenitors from the blood into the infected site, where a PAMP (Flagellin) stimulates these progenitors via their own PRR (TLR5) to spin off MΦ progeny (Fig. 5G). Upon i.n. administration, Flagellin mainly remains localized in the lung[9]. Consistently, we observed in our experiments that Flagellin promoted M8 differentiation in the lung, but not in blood or BM. Intraperitoneal injection of Flagellin was shown earlier to result in proliferation of myeloid primed progenitor cells, termed MMP3 cells ($Lin^{-}Sca\text{-}1^{+}c\text{-}Kit^{+}Flt\text{-}3^{-}CD150^{-}CD48^{+}$)[22], which are distinct from MO(D)P. It was not examined whether these cells expressed TLR5. To our knowledge, we are the first to report TLR5 expression on hematopoietic progenitors. Flagellin promoted MΦ differentiation from MO(D)P, but not OC differentiation. Flagellin has been reported to promote OC formation in assays with whole bones, but in agreement with our findings, it did not affect RANKL/M-CSF-induced OC differentiation from progenitors[39].

In our *in vivo* setting, we transferred MOP i.v. to mimic the physiological situation, in which progenitors circulate between blood and BM[38]. We could not trace the adoptively transferred MOP back to the lung, but we did detect their MΦ offspring. In addition, we detected recruitment of endogenous MOP of the recipient mice into the lung in response to Flagellin inoculation. We considered that MOPs might be attracted from the blood into the lung by CCL2, because lung epithelial cells secrete CCL2 in response to Flagellin[33, 34] and CCL2 is important to attract monocytes into tissue[5]. Also, CCR2 is important for the trafficking of hematopoietic cells to sites of inflammation[40]. CCR2 expression was higher on the MΦ/OC committed MOP than on the upstream MODP, which is in line with earlier findings that CCR2 expression on HSPC progressively increases from self-

renewing HSC, to MPP, to specialized myeloid progenitors CMP and GMP[40]. *In vitro,* type 2 AEC produced more CCL2 upon stimulation with Flagellin. We also found that LLF from Flagellin-treated mice attracted more MOPs than did LLF from PBS-treated mice, which relied on CCR2. These data suggest that CCL2 from Flagellin-stimulated AEC led to the recruitment of MOP into the lung (Fig. 5G). This possibility can be further addressed by in vivo blockade of the CCL/CCR2 axis.

Interestingly, it has also been reported that hematopoietic progenitor cells can migrate at steady state from blood into a diversity of peripheral tissues[41]. Accordingly, we found endogenous MOP in lungs of CD45.2 recipient mice in absence of Flagellin inoculation. Therefore, the presence of PRR on these progenitors may enable them to directly sense pathogens in infected tissue and spin off progeny locally when the appropriate differentiation factors are present. This may be the earliest effect on progenitors during infection and may be followed by progressive recruitment of progenitors into the tissue for amplification of the response.

In summary, we here provide evidence for a scenario in which Flagellin-sensing by lung epithelial cells leads to a rapid influx of MΦ/OC progenitors from the circulation and Flagellin sensing by these progenitors promotes local MΦ differentiation. We suggest that this type of emergency myelopoiesis enables quick and qualified phagocyte replenishment, representing another layer of host protection against bacterial infections at mucosal sites. Future studies should address whether TLR5-mediated MΦ differentiation from myeloid progenitors promotes host protection against bacterial infection.

Materials and methods

Mice

Wild-type (WT) CD45.1 and CD45.2 C57BL/6 mice of 6–12 weeks of age were used for in vitro or in vivo experiments. For *in vivo* experiments, age-matched female mice were used. For *in vitro* and *ex vivo* experiments, male and female mice were used at random. Experiments were performed in accordance with national guidelines and approved by the Experimental Animal Committee of The Netherlands Cancer Institute.

Isolation of BM mononuclear cells

Tibiae, femurs and ilia were washed with phosphate buffered saline (PBS) and ground in a mortar in presence of PBS. BM cells were flushed out of the bone fragments with RPMI-1640 medium (Gibco, Life Technologies) with 10% fetal calf serum (FCS) and

the cell suspension was forced through a 70μm cell strainer to remove bone chips and other debris. Cells were recovered by centrifugation and erythrocytes were removed with eBioscienceTM red blood cell lysis buffer. After incubation on ice for 1–2min, RPMI-1640 medium with 10% FCS was added and BM cells were collected by centrifugation and resuspended in medium until further use.

Intranasal Flagellin administration and adoptive cell transfer

MOP from pooled BM of CD45.1 female donor mice (n = 5) were flow cytometrically sorted and transferred intravenously (i.v.) via the retro-orbital plexus into age-matched female CD45.2 recipient mice (n = 8) at 100,000 cells in 200 μl PBS per mouse. At 24 h after adoptive transfer, recipient mice were anesthetized by methoxyflurane inhalation, and intranasally (i.n.) inoculated with 1 μg Flagellin (Invitrogen) in 50 μl PBS per mouse (n = 4) or with 50 μl PBS (n = 4).

Lung Lavage Fluid

Mice were i.n. inoculated with 1 μg Flagellin in 50 μl PBS (n = 4) or PBS only (n = 3). At 3–4 h after inoculation, mice were sacrificed and lungs together with intact tracheae were harvested. 200 μl PBS was injected into the trachea with a 1ml syringe with a blunted 25 gauge needle until all lobes of the lung were bloated. The lung was flushed three times with the PBS while the needle was fixed in the trachea. Next, the liquid in the syringe was harvested as LLF.

Cell isolation from lung for CCL2 detection

Lungs were minced into small pieces (<0.5 mm3) and incubated in 5ml of 200 mg/ml Liberase TL Research Grade (Sigma- Aldrich) at 37◦C for 15min. Cells were liberated from tissue by continuously pipetting the sample for 15min at room temperature. Cells were filtered through a 40 μm strainer (BD Biosciences) and washed twice with RPMI-1640 containing 0.01% deoxyribonuclease I (DNase, Sigma-Aldrich). After red blood cell lysis, cells were plated in non-adherent round-bottom 96-well plates (BD Falcon) at a density of 300,000 cells/well and subsequently treated with or without Flagellin (100 ng/ml) in RPMI-1640 medium with 1% FCS. Protein transport inhibitor (GolgiPlug, BD Biosciences) was added to the cultures at a concentration of 1:1,000 and 12 h later, cells were harvested, stained for CD45, MHC-II, CD31, and CCL2 and analyzed by flow cytometry.

Flow cytometry

For isolation of M8/OC progenitor cell populations, mouse BM cells were incubated with the identifying antibodies (Table S1) in cell staining buffer (Biolegend) for 45min on ice. Dead cells were excluded by staining with 7-amino-actinomycin D (7-AAD) or 4,6-Diamidino-2- Phenylindole (DAPI). In order to prevent clump formation from dead cells, 0.01% DNase was added. Cell sorting was performed on BD FACSAriaTM Fusion (BD Biosciences). For analysis, *ex vivo* cells and in vitro cultured cells in mouse experiments were stained with indicated antibodies (Table S1) in cell staining buffer for 45min on ice and analyzed on a BDTM LSR II SORP, BD LSRFortessaTM, or BD FACSymphonyTM A5 SORP flow cytometer (BD Biosciences). Fluorescence minus one (FMO) was used as negative control where indicated. Data were analyzed with FlowJoTM software (BD). The gating strategy for identifying MODP and MOP populations in relation to other HSC populations is shown in Figure S1. The same gating strategy has been used throughout this study to identify MODP and MOP populations. For analysis of all other cell populations, gating strategies are provided in the figures. For detection of c-Fms (CD115) cell surface expression, we originally used direct ex vivo staining, but later preincubated the BM cells overnight in culture medium at 37◦C, 5% CO2 prior to staining, which enhanced the signal (Figures S1, 4, 9).

In vitro Differentiation of mouse progenitors into OC, MΦ, and DC

MODP and MOP cell populations were sorted by flow cytometry and seeded in 96-well plates (BD Falcon) (flat bottom for OC differentiation, round bottom for MΦ and DC differentiation) at 2,000–3,000 cells/well. To induce OC differentiation, progenitor cells were cultured in a minimum essential medium (α-MEM; Gibco, Life Technologies) with 10% FCS, supplemented with 20 ng/ml recombinant mouse (rm) RANK ligand (RANKL, R&D) and 25 ng/ml rm macrophage colony-stimulating factor (M-CSF) (Peprotech). To induce MΦ differentiation, progenitor cells were cultured in IMDM with 10% FCS, supplemented with 25 ng/ml rm M-CSF. To induce DC differentiation, progenitor cells were cultured in IMDM with 10% FCS, supplemented with 200 ng/ml rm FLT3 ligand (R&D). Flagellin (0.5μg/ml; Invitrogen) was added into cultures as specified. OC differentiation was assessed by tartrate-resistant acid phosphatase (TRAP) staining (Sigma-Aldrich) according to manufacturer's instructions after 6 days of culture. Cells were washed with PBS, fixed with paraformaldehyde (PFA; Sigma-Aldrich) for 15min at RT. Fixed cells were washed twice with pre-warmed water to remove remaining PFA.

Next, cells were incubated with TRAP staining solution for 5–10min at RT and washed according to manufacturer's instructions. $TRAP^+$ OC were analyzed by light microscopy (Nikon) and quantified using ImageJ (National Institutes of Health).

In vitro transwell migration assay

Total BM cells or sorted progenitors were plated at equal numbers (100,000 cells per well or 5,000 cells per well, respectively) in the upper chamber of a 24-well or a 96-well HTS 3μm polycarbonate transwell plate (Corning) in 100 μl serumfree IMDM (Gibco, Life Technologies). Sorted progenitors were seeded in the presence or absence of CCR2 blocking mAb (0.75μM; Tocris). The lower chambers contained 300 μl LLF from PBS-, or Flagellin-treated mice. After 12 h, cells that had migrated into lower chambers were collected, stained with antibodies and analyzed by flow cytometry.

Statistical analysis

Statistical evaluation was performed in GraphPad Prism 8 (GraphPad Software, Inc.) using unpaired two-tailed Student's t-test or one way ANOVA test.

Data availability statement

The datasets presented in this study can be found in online repositories. The name of the repository and accession number can be found here: NCBI (accession: GSE97380).

Ethics statement

The animal study was reviewed and approved by the IVD of the Netherlands Cancer Institute.

Acknowledgements

This work was supported by the Landsteiner Foundation for Blood Research grant 1355 (to YX and JB) and a postdoctoral fellowship from the Foundation AlfonsoMartín Escudero (to JP). We thank F. van Diepen from the flow cytometry facility at the Netherlands Cancer Institute for support in cell sorting and staff from the animal core facility at the Netherlands Cancer Institute for mouse care. We thank Dr. A. F. de Vos and Prof. W. J.Wiersinga from the Center for Experimental and Molecular Medicine at the Amsterdam University Medical Center for providing us BM cells from *Tlr5*$^{-/-}$ and *Tlr5*+/+ littermate mice.

Author contributions

YX designed the research, designed and performed animal experiments, analyzed and interpreted data, and wrote the manuscript. JB designed the research, interpreted data, and wrote the manuscript. XL and JP designed and performed experiments, analyzed data, and wrote the manuscript. TW contributed to experiments. MB advised on flow cytometry and contributed to cell sorting. IR contributed to data analysis. All authors contributed to the article and approved the submitted version.

References

1. Eisele NA, Anderson DM. Host defense and the airway epithelium: frontline responses that protect against bacterial invasion and pneumonia. J Pathog. (2011) 2011:249802. doi: 10.4061/2011/249802
2. Günther J, Seyfert HM. The first line of defence: insights into mechanisms and relevance of phagocytosis in epithelial cells. Semin Immunopathol. (2018) 40:555–65. doi: 10.1007/s00281-0180701-1
3. Guilliams M, Thierry GR, Bonnardel J, Bajenoff M. Establishment and maintenance of the macrophage niche. Immunity. (2020) 52:434–51. doi: 10.1016/j.immuni.2020.02.015
4. Ginhoux F, Jung S. Monocytes and macrophages: developmental pathways and tissue homeostasis. Nat Rev Immunol. (2014) 14:392–404. doi: 10.1038/nri3671
5. Shi C, Pamer EG. Monocyte recruitment during infection and inflammation. Nat Rev Immunol. (2011) 11:762–74. doi: 10.1038/nri3070
6. Akira S, Takeda K. Toll-like receptor signalling. Nat Rev Immunol. (2004) 4:499–511. doi: 10.1038/nri1391
7. Hayashi F, Smith KD, Ozinsky A, Hawn TR, Yi EC, Goodlett DR, et al. The innate immune response to bacterial flagellin is mediated by Toll-like receptor 5. Nature. (2001) 410:1099–103. doi: 10.1038/35074106
8. Vijayan A, RumboM, Carnoy C, Sirard JC. Compartmentalized antimicrobial defenses in response to flagellin. Trends Microbiol. (2018) 26:423–35. doi: 10.1016/j.tim.2017.10.008
9. Van Maele L, Fougeron D, Janot L, Didierlaurent A, Cayet D, Tabareau J, et al. Airway structural cells regulate TLR5-mediated mucosal adjuvant activity. Mucosal Immunol. (2014) 7:489–500. doi: 10.1038/mi.2013.66
10. Honko AN, Mizel SB. Effects of flagellin on innate and adaptive immunity. Immunol Res. (2005) 33:83–101. doi: 10.1385/ir:33:1:083
11. Gewirtz AT, Simon PO, Schmitt CK, Taylor LJ, Hagedorn CH, O'Brien AD, et al. Salmonella typhimurium translocates flagellin across intestinal epithelia, inducing a proinflammatory response. J Clin Invest. (2001) 107:99–109. doi: 10.1172/JCI10501
12. Zeng H, Carlson AQ, Guo Y, Yu Y, Collier-Hyams LS, Madara JL, et al. Flagellin is the major proinflammatory determinant of enteropathogenic Salmonella. J Immunol. (2003) 171:3668–74. doi: 10.4049/jimmunol.171.7.3668
13. Eaves-Pyles T, Murthy K, Liaudet L, Virág L, Ross G, Soriano FG, et al. Flagellin, a novel mediator of Salmonella-induced epithelial activation and systemic inflammation: IkBa degradation, induction of nitric oxide synthase, induction of proinflammatory mediators, and cardiovascular dysfunction. J Immunol. (2001) 166:1248–60. doi: 10.4049/jimmunol.166.2.1248
14. Means TK, Hayashi F, Smith KD, Aderem A, Luster AD. The Toll-like receptor 5 stimulus bacterial flagellin induces maturation and chemokine production in human dendritic cells. J Immunol. (2003) 170:5165–75. doi: 10.4049/jimmunol.170.10.5165
15. Sanders CJ, Moore DA, Williams IR, Gewirtz AT. Both radioresistant and hemopoietic cells promote innate and adaptive immune responses to flagellin. J Immunol. (2008) 180:7184–92. doi: 10.4049/jimmunol.181.4.2933

16. Uematsu S, Jang MH, Chevrier N, Guo Z, Kumagai Y, Yamamoto M, et al. Detection of pathogenic intestinal bacteria by Toll-like receptor 5 on intestinal CD11c+ lamina propria cells. Nat Immunol. (2006) 7:868–74. doi: 10.1038/ni1362

17. Lodes MJ, Cong Y, Elson CO, Mohamath R, Landers CJ, Targan SR, et al. Bacterial flagellin is a dominant antigen in Crohn disease. J Clin Invest. (2004) 113:1296–306. doi: 10.1172/JCI200420295

18. Mizel SB, Bates JT. Flagellin as an adjuvant: cellular mechanisms and potential. J Immunol. (2010) 185:5677–82. doi: 10.4049/jimmunol.1002156

19. Nagai Y, Garrett KP, Ohta S, Bahrun U, Kouro T, Akira S, et al. Toll-like receptors on hematopoietic progenitor cells stimulate innate immune system replenishment. Immunity. (2006) 24:801–12. doi: 10.1016/j.immuni.2006.04.008

20. Capitano ML. Toll-like receptor signaling in hematopoietic stem and progenitor cells. Curr Opin Hematol. (2019) 26:207–13. doi: 10.1097/MOH.0000000000000511

21. Sioud M. Microbial sensing by hematopoietic stem and progenitor cells: vigilance against infections and immune education of myeloid cells. Scand J Immunol. (2020) 92:e12957. doi: 10.1111/sji.12957

22. Zhang B, Oyewole-Said D, Zou J, Willliams IR, Gewirtz AT. TLR5 signaling in murine bone marrow induces hematopoietic progenitor cell proliferation and AIDS survival from radiation. Blood Adv. (2017) 1:1796–806. doi: 10.1182/bloodadvances.2017006981

23. Boettcher S, Manz MG. Regulation of inflammation- and infection-driven hematopoiesis. Trends Immunol. (2017) 38:345–57. doi: 10.1016/j.it.2017.01.004

24. Xiao Y, Song J-Y, de Vries TJ, Fatmawati C, Parreira DB, Langenbach GEJ, et al. Osteoclast precursors in murine bone marrow express CD27 and are impeded in osteoclast development by CD70 on activated immune cells. Proc Natl Acad Sci USA. (2013) 110:12385–90. doi: 10.1073/pnas.1216082110

25. Xiao Y, Zijl S, Wang L, De Groot DC, Van Tol MJ, Lankester AC, et al. Identification of the common origins of osteoclasts, macrophages, and dendritic cells in human hematopoiesis. Stem Cell Rep. (2015) 4:984–94. doi: 10.1016/j.stemcr.2015.04.012

26. Xiao Y, Palomero J, Grabowska J, Wang L, de Rink I, van Helvert L, et al. Macrophages and osteoclasts stem from a bipotent progenitor downstream of a macrophage/osteoclast/dendritic cell progenitor. Blood Adv. (2017) 1:1993–2006. doi: 10.1182/bloodadvances.2017008540

27. Mansour A, Abou-Ezzi G, Sitnicka E, Jacobsen SEW, Wakkach A, Blin-Wakkach C. Osteoclasts promote the formation of hematopoietic stem cell niches in the bone marrow. J Exp Med. (2012) 209:537–49. doi: 10.1084/jem.20110994

28. Jung YK, Kang YM, Han S. Osteoclasts in the inflammatory arthritis: implications for pathologic osteolysis. Immune Netw. (2019) 19:e2. doi: 10.4110/in.2019.19.e2

29. Tanaka Y, Nakayamada S, Okada Y. Osteoblasts and osteoclasts in bone remodeling and inflammation. Curr Drug Targets Inflamm Allergy. (2005) 4:325–8. doi: 10.2174/1568010054022015

30. Weissman IL, Shizuru JA. The origins of the identification and isolation of hematopoietic stem cells, and their capability to induce donor-specific transplantation tolerance and treat autoimmune diseases. Blood. (2008) 112:3543–53. doi: 10.1182/blood-2008-08-078220

31. Lacey DL, Timms E, Tan HL, Kelley MJ, Dunstan CR, Burgess T, et al. Osteoprotegerin ligand is a cytokine that regulates osteoclast differentiation and activation. Cell. (1998) 93:165–76. doi: 10.1016/S0092-8674(00)81569-X

32. Raoust E, Balloy V, Garcia-Verdugo I, Touqui L, Ramphal R, Chignard M. Pseudomonas aeruginosa LPS or flagellin are sufficient to activate TLR dependent signaling in murine alveolar macrophages and airway epithelial cells. PLoS ONE. (2009) 4:e7259. doi: 10.1371/journal.pone.0007259

33. Becker S, Quay J, Koren HS, Haskill JS. Constitutive and stimulated MCP-1, GROa, b, and g expression in human airway epithelium and bronchoalveolar macrophages. Am J Physiol Lung CellMol Physiol. (1994) 266(3 Pt 1):L278–86. doi: 10.1152/ajplung.1994.266.3.L278

34. Clark JG, Kim KH, Basom RS, Gharib SA. Plasticity of airway epithelial cell transcriptome in response to flagellin. PLoS ONE. (2015) 10:e0115486. doi: 10.1371/journal.pone.0115486

35. Bello-Irizarry SN, Wang J, Olsen K, Gigliotti F, Wright TW. The alveolar epithelial cell chemokine response to Pneumocystis requires adaptor molecule MyD88 and interleukin-1 receptor but not toll-like receptor 2 or 4. Infect Immun. (2012) 80:3912–20. doi: 10.1128/IAI.00708-12

36. Hasegawa K, Sato A, Tanimura K, Uemasu K, Hamakawa Y, Fuseya Y, et al. Fraction of MHCII and EpCAM expression characterizes distal lung epithelial cells for alveolar type 2 cell isolation. Respir Res. (2017) 18:150. doi: 10.1186/s12931-017-0635-5

37. Takizawa H, Boettcher S, Manz MG. Demand-adapted regulation of early hematopoiesis in infection and inflammation. Blood. (2012) 119:2991–3002. doi: 10.1182/blood-2011-12-380113

38. Mazo IB, Massberg S, von Andrian UH. Hematopoietic stem and progenitor cell trafficking. Trends Immunol. (2011) 32:493–503. doi: 10.1016/j.it.2011.06.011

39. Kassem A, Henning P, Kindlund B, Lindholm C, Lerner UH. TLR5, a novel mediator of innate immunity-induced osteoclastogenesis and bone loss. FASEB J. (2015) 29:4449–60. doi: 10.1096/fj.15-272559

40. Si Y, Tsou CL, Croft K, Charo IF. CCR2 mediates hematopoietic stem and progenitor cell trafficking to sites of inflammation in mice. J Clin Invest. (2010) 120:1192–203. doi: 10.1172/JCI40310

41. Massberg S, Schaerli P, Knezevic-Maramica I, Köllnberger M, Tubo N, Moseman EA, et al. Immunosurveillance by hematopoietic progenitor cells trafficking through blood, lymph, and peripheral tissues. Cell. (2007) 131:994– 1008. doi: 10.1016/j.cell.2007.09.047

Supplementary information

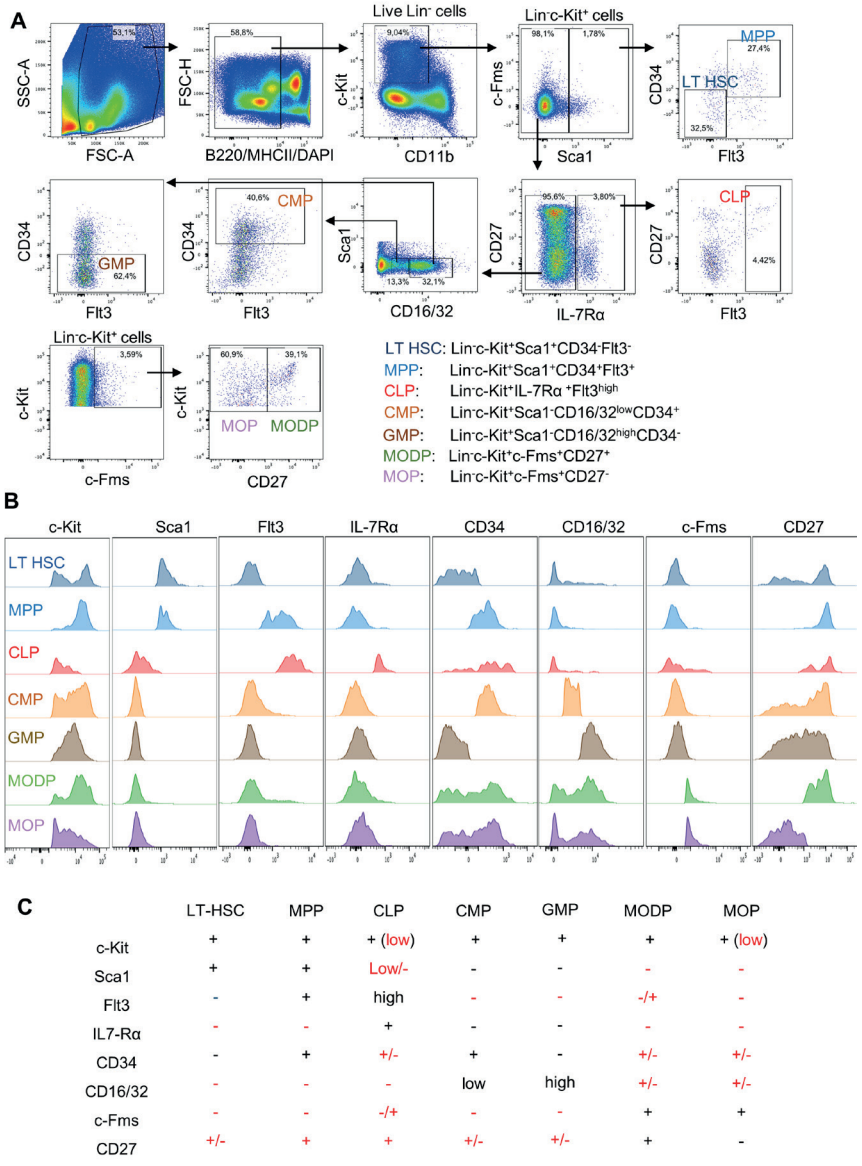

Fig. S1 Cell surface phenotype of MODP, MOP and other progenitors. BM cells were simultaneously stained with antibodies detecting MODP and MOP and all characteristic progenitor markers indicated. (**A**) Gating strategy of live (DAPI$^-$) B220$^-$MHCII$^-$CD11b$^{low/-}$c-Kit$^+$ mouse BM cells (G1) and its further separation into long term (LT)-HSC, MPP, CLP, CMP, GMP as defined by the indicated cell surface markers defined in ref. 30, as well as MODP and MOP as defined in ref. 26. (**B**) Histograms depicting the cell surface expression of the indicated markers on the indicated progenitor populations. (**C**) Overview of the defining markers for the indicated progenitor populations according to refs. 26 and 30 (black) and according to this flow cytometric analysis (red). Data are representative of 2 experiments with 2 mice each.

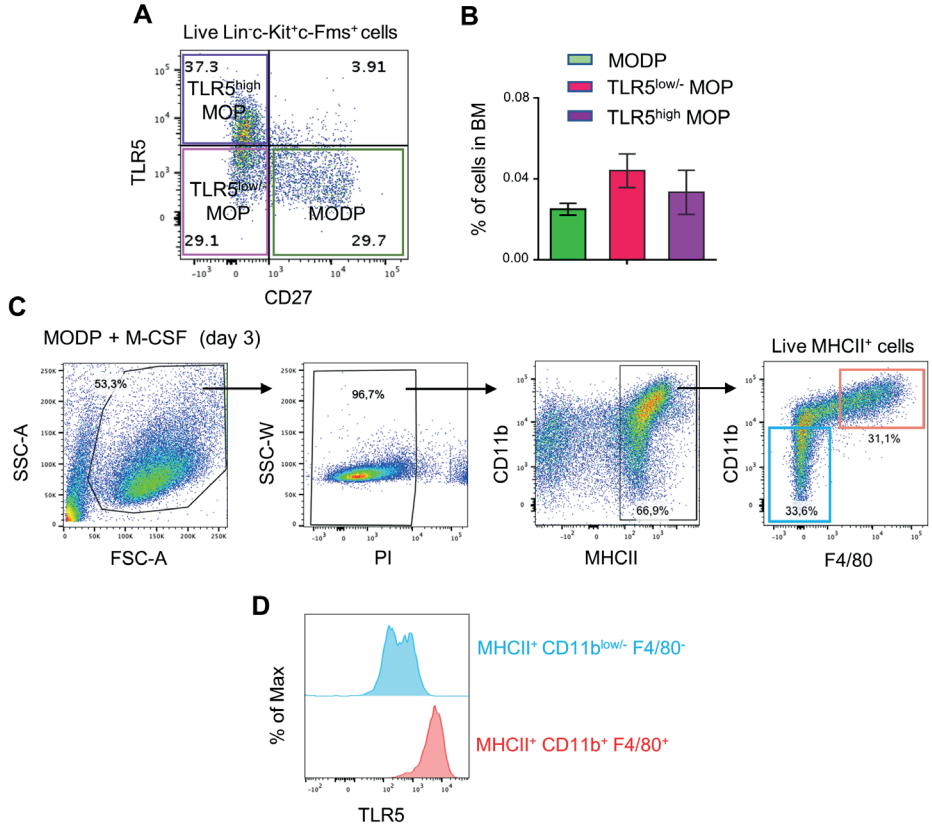

Fig. S2 Identification of TLR5$^{low/-}$and TLR5^{high} MOP in BM and TLR5 detection on offspring of the MODP in MΦ differentiation culture. (A) Representative flow cytometry plot depicting the gating strategy to distinguish MODPs, TLR5$^{low/-}$ and TLR5^{high} MOP in live Lin^{-}c-Kit^{+}c-Fms^{+} BM cells. (B) Bar chart depicting the frequencies (%) of MODP, TLR5$^{low/-}$ and TLR5^{high} MOP among total live cells in BM, as diagnosed by flow cytometry. Data is pooled from three independent experiments with technical duplicates of pooled BM cells from two mice (error bars indicate SD). (C-D) MODP were seeded at 2,000 cells/well and cultured with M-CSF. After 3 days, offspring cells were analyzed by flow cytometry. (C) Representative flow cytometry plots depicting the gating strategy for MHCII^{+}CD11b^{+}F4/80^{+} and MHCII^{+}CD11b$^{low/-}$F4/80^{-} cell populations in the culture. (D) Histogram depicting TLR5 cell surface expression on the indicated populations. Data are representative of three independent experiments. In each experiment, MODP were sorted from pooled BM cells from 3-4 mice and technical duplicates were used for differentiation cultures.

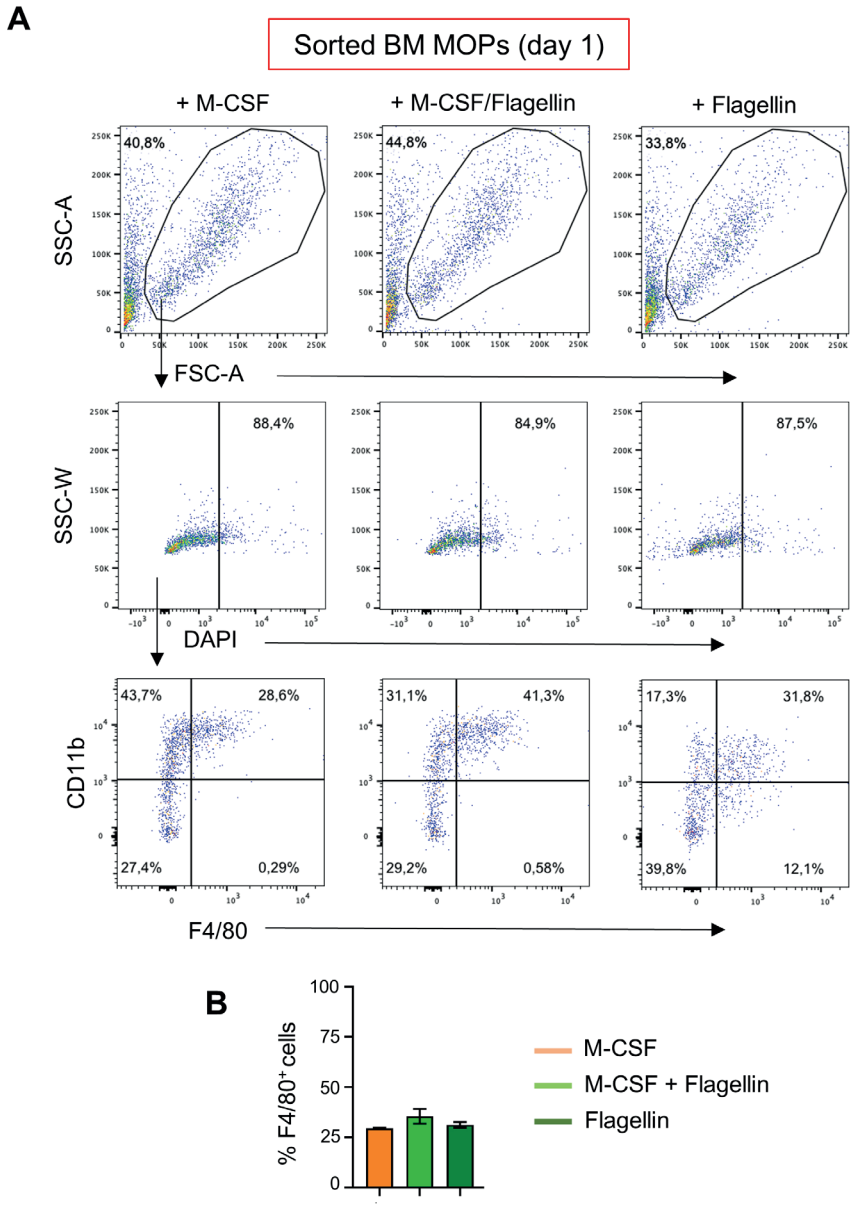

Figure S3. Gating strategy and quantification of MOP offspring cells in in vitro MΦ differentiation culture at day 1. MOP were seeded at 2,000 cells/well and cultured with M-CSF with or without Flagellin, or with Flagellin only. Offspring cells were analyzed by flow cytometry after 1 day of culture. (**A**) Representative flow cytometry plots depicting gating strategy for MΦ, defined as $MHCII^+CD11b^+F4/80^+$ cells. (**B**) Bar chart depicting frequencies (%) of $F4/80^+$ cells in the $MHCII^+CD11b^+$ gate. Data are representative of two independent experiments, in which MOP were sorted from pooled BM cells from 3-4 mice and technical duplicates were used for differentiation cultures. Error bars indicate SEM.

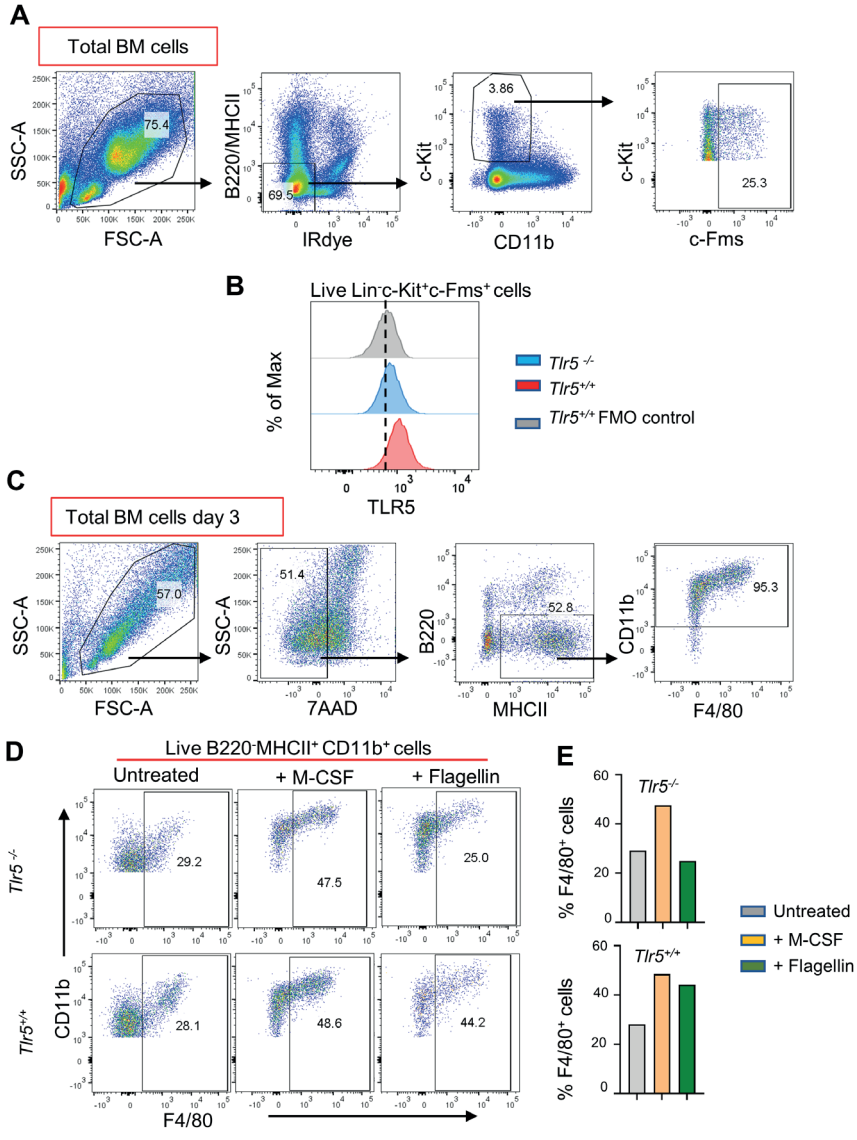

Figure S4. TLR5 staining and MΦ differentiation assay of Tlr5$^{-/-}$ and Tlr5$^{+/+}$ BM cells. (A-B) BM cells from Tlr5$^{-/-}$ and Tlr5$^{+/+}$ mice were stained for TLR5 in combination with progenitor markers and analyzed by flow cytometry. (**A**) Representative flow cytometry plots depicting gating strategy for Lin^{-}c-Kit^{+}c-Fms^{+} cells. (**B**) Histograms depicting TLR5 cell surface staining on Lin^{-}c-Kit^{+}c-Fms^{+} cells from Tlr5$^{-/-}$ (n=1) and Tlr5$^{+/+}$ (n=1) BM samples. TLR5 FMO control was from Tlr5$^{+/+}$ BM sample. Data is from one experiment with technical duplicates. (**C-E**) Total Tlr5$^{-/-}$ and Tlr5$^{+/+}$ BM cells were plated at density of 200,000 cells/well and cultured with M-CSF or Flagellin or medium only (untreated) and 3 days later the cultures were analyzed by flow cytometry. (**C-D**) Representative flow cytometry plots depicting the gating strategy for MΦ, defined as MHCII^{+}CD11b^{+}F4/80^{+} cells. (**E**) Frequencies (%) of F4/80^{+} cells within live B220^{-} MHCII^{+}CD11b^{+} cells in the MΦ cultures from Tlr5$^{-/-}$ and Tlr5$^{+/+}$ BM cells.

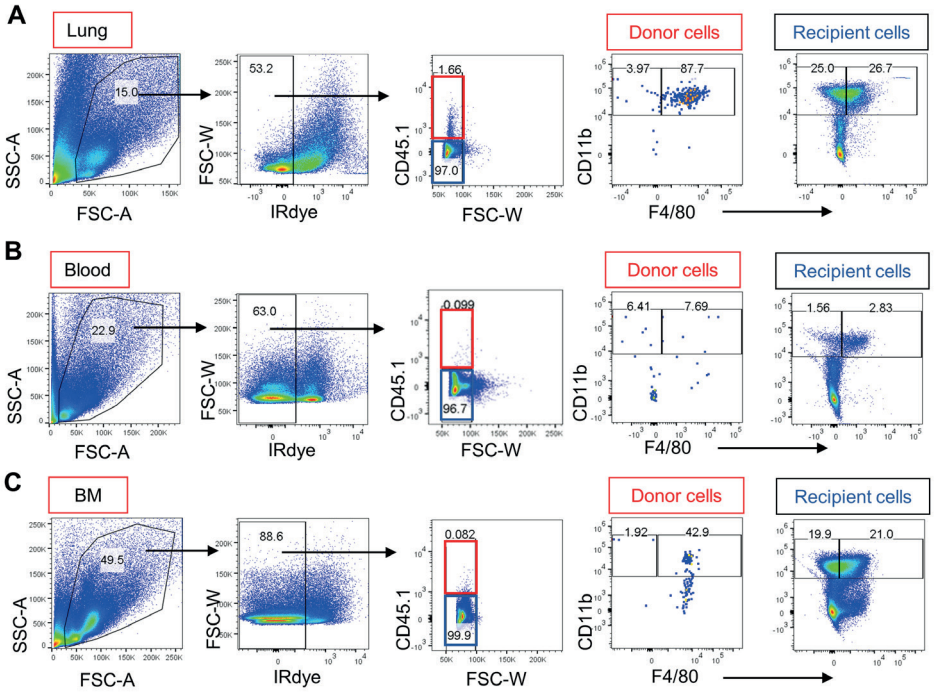

Figure S5. Gating strategy for MΦ from i.v. transferred CD45.1+ donor cells CD45.1- recipient cells. MOP ($Lin^{-}c\text{-}Kit^{+}c\text{-}Fms^{+}CD27^{low/-}$) were flow cytometrically sorted from pooled BM cells of CD45.1 donor mice (n=5) and intravenously (i.v.) transferred into CD45.2 recipient mice. At 24 h after adoptive cell transfer, 1 µg Flagellin in 50 µl PBS or 50 µl PBS was inoculated intranasally (i.n.) into the recipient mice. 24 hours after i.n. inoculation, lung, blood and BM were harvested and dissociated into single cells for flow cytometric analysis (as described in Fig. 4). (**A-C**) Representative flow cytometry plots depicting gating strategy for MΦ, defined as $MHCII^{+}CD11b^{+}F4/80^{+}$ cells among $CD45.1^{+}$ donor cells and $CD45.1^{-}$ recipient cells in the lung, blood and BM respectively. Data are representative of two independent experiments each with n=4 recipient mice per group.

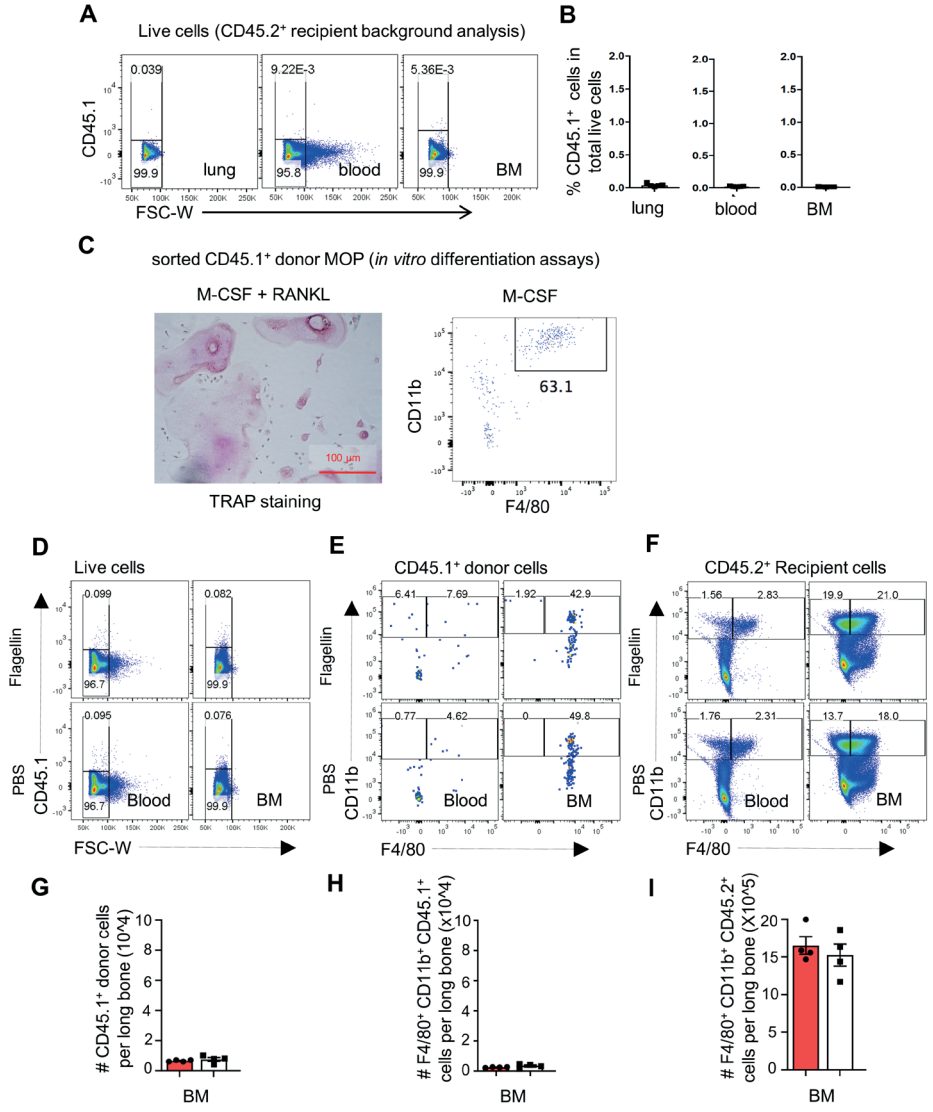

Figure S6. MΦ differentiation from i.v. transferred MOP in blood and BM. (**A**) CD45.2 mice that did not receive cells or treatment were used for background analysis. Representative flow cytometry plots depicting frequencies (%) of cells staining with antibody to CD45.1 in lung, blood and BM. (**B**) Quantification of background CD45.1 staining. Data is from one experiment with 3 mice. (**C**) In vitro evaluation at day 5 of OC and MΦ differentiation potential of CD45.1$^+$ MOP prior to adoptive transfer. Light microscopic image (left) depicting TRAP-stained cells in OC culture and flow cytometry plot (right) depicting frequencies (%) of MΦ, defined as MHCII$^+$CD11b$^+$F4/80$^+$ cells in the MΦ culture. (**D-F**) Representative flow cytometry plots depicting adoptively transferred CD45.1$^+$ cells, CD45.1$^+$ MOP-derived MΦ and CD45.1$^-$ endogenous MΦ in blood and BM. (**G-I**) Quantification of CD45.1$^+$ cells, CD45.1$^+$ MOP-derived MΦ and CD45.1$^-$ endogenous MΦ in BM, as indicated by absolute numbers (#) per long bone. Data are representative of two independent experiments with n=4 each. Error bars indicate SEM, and unpaired two tailed Student's t test was used for statistical evaluation.

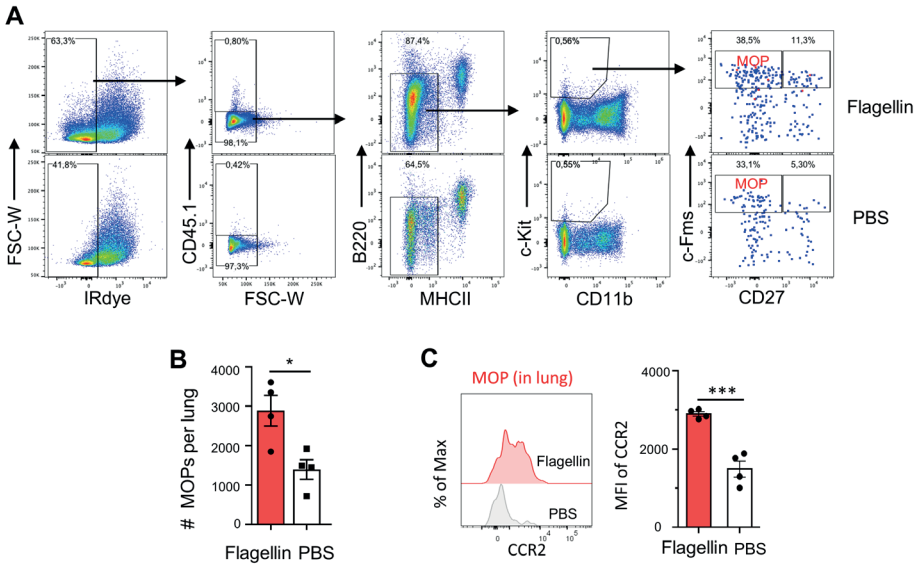

Figure S7. Detection of CD45.1$^-$ recipient MOP and their CCR2 expression in the lung. (A-D) Lung single-cell suspensions from mice that had been inoculated i.n. with Flagellin or PBS (as described in Figure 4) were stained with antibody to CCR2 in combination with antibodies to MOP markers and analyzed by flow cytometry. (**A**) Representative flow cytometry plots depicting gating strategy for CD45.1$^-$ MOP in the lung from mice that had received i.n. Flagellin or PBS. (**B**) Quantification of CD45.1$^-$ MOP in the lung, as indicated by absolute numbers (#). (**C**) Cell surface detection of CCR2 by flow cytometry on MOP in the lung from mice that had received i.n. Flagellin or PBS as indicated by histogram (left) and MFI (right). Data are representative of two independent experiments with n=4 for S7A, B. Data are from one experiment with n=4 for S7C. Error bars indicate SEM, and unpaired two tailed Student's t test was used for statistical evaluation.

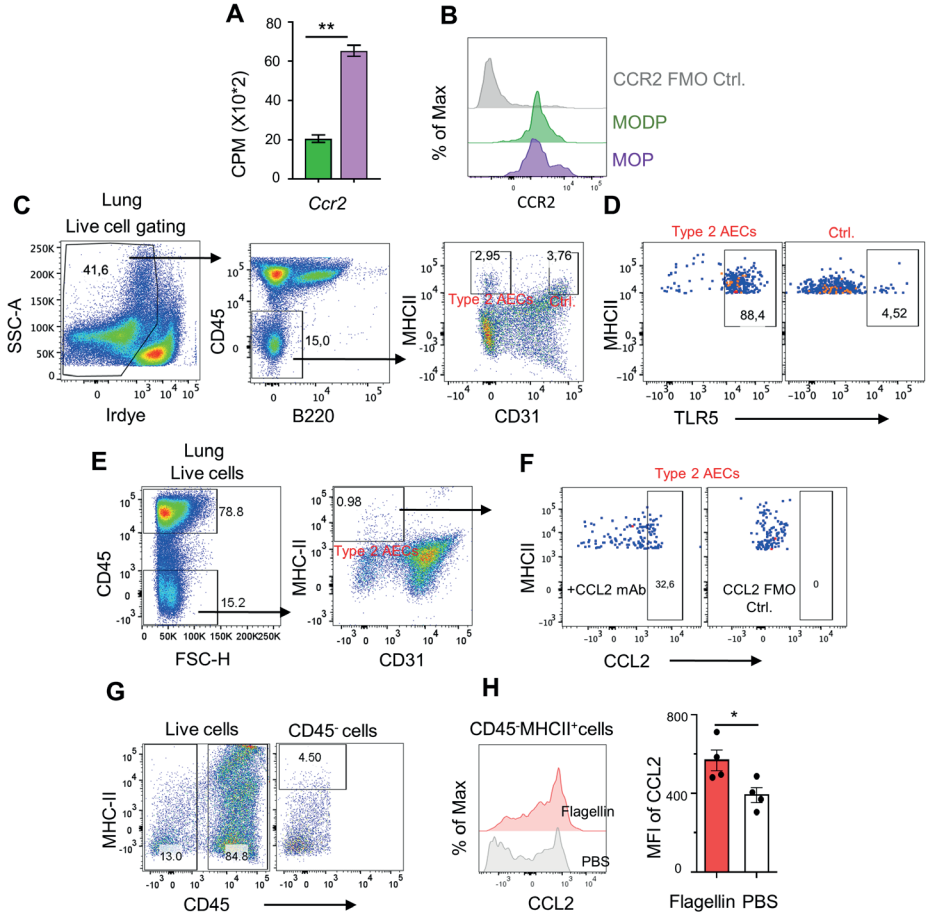

Figure S8. Detection of CCR2 in MODP and MOP in BM at transcript and protein level, and detection of CCL2 and TLR5 in type 2 AEC in lung. (A) Ccr2 mRNA levels in MODP and MOP based on normalized read counts (CPM) (n=3), as determined by transcriptomics (GSE97380;(26)) (see legend to Figure 1D). (B) Histogram depicting flow cytometric detection of CCR2 on MODP and MOP populations in mouse BM. CCR2 FMO was used as control. Data are representative of two independent experiments with n=2. (C, D) Single-cell suspensions of lung tissue were stained to detect TLR5 and type 2 AEC by flow cytometry. Representative flow cytometry plots depicting gating strategy for live type 2 AEC defined as $CD45^-MHCII^+CD31^-$ cells (C) and cell surface expression of TLR5 on type 2 AEC (D). $CD45^-MHCII^+CD31^+$ cells were used as controls (Ctrl.). (E, F) Single-cell suspensions of lung tissue were cultured in medium with or without Flagellin overnight, stained for CCL2 (intracellularly) and type 2 AEC markers and analyzed by flow cytometry. Flow cytometry plots depicting gating strategy for live type 2 AEC defined as $CD45^-MHCII^+CD31^-$ cells. (E) and intracellular CCL2 expression in type 2 AEC (F). CCL2 FMO was used as control. For statistical information for panels C-F, see Fig. 5B. (G,H) Lung single-cell suspensions from mice that had been inoculated i.n. with Flagellin or PBS (as described in Figure 4) were stained with antibody to CCL2 (intracellular) in combination with antibodies to CD45 and MHCII, and analyzed by flow cytometry. (G) Representative flow cytometry plots depicting gating strategy for $CD45^-MHCII^+$ non-hematopoietic cells in the lung tissues. (H) Plots depicting CCL2 detection by intracellular staining in $CD45^-MHCII^+$ non-hematopoietic cells in histogram (left) and MFI (right). CCL2 FMO was used as control. MFI was calculated as median value of the fluorescent staining. For statistical information for panels G, H, see Fig. 4.

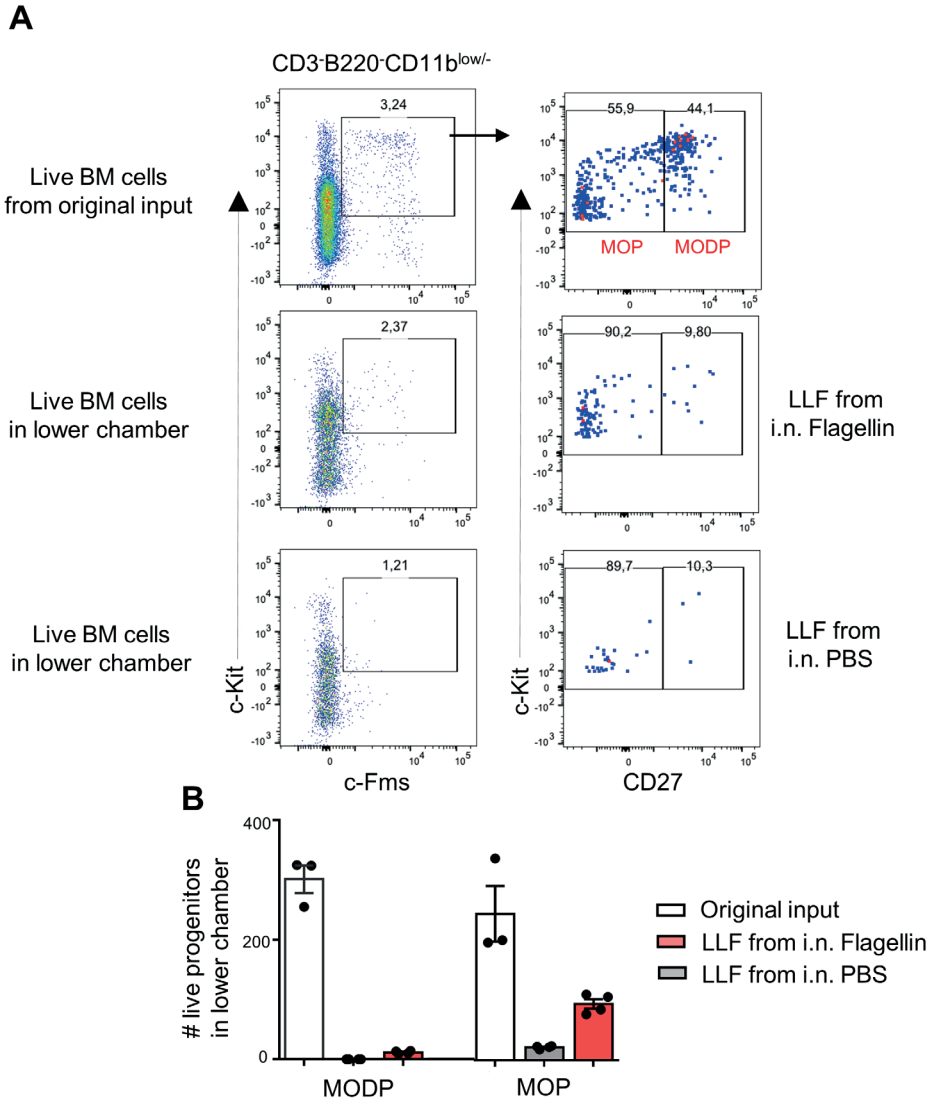

Figure S9. Detection of MODP and MOP migration. LLF was harvested as described in Materials and Methods from the two groups of mice that had been used for the in vivo experiments. LLF was placed in the lower chambers of transwell plates. In the upper chambers, pooled BM cells from three mice were seeded at density of 100,000 cells per well. 100,000 total BM cells per well were directly placed in the lower chambers of transwell plates to obtain the original input information. After 12 h of incubation, cells in the lower chambers were collected for phenotyping and quantification by flow cytometry. (**A**) Representative flow cytometry plots depicting the gating strategy for B220^{-}CD11b$^{low/-}$c-Kit^{+}c-Fms^{+} CD27^{high} MODP and CD27$^{low/-}$ MOP in the lower chambers. (**B**) Bar chart depicting total live cell number (#) of MODP and MOP as original input and total live cell numbers of MODP and MOP that migrated into the lower chambers. Data are representative of two independent experiments and each experiment includes LLF from n=3-4. Error bars indicate SEM.

Table S1. Antibody and reagent list

Antibody	Fluorochrome	Clone	Manufacturer	Catalogue
CD3 #	AF488	17A2	BioLegend	100210
CD11b *#	BV786	M1/70	BioLegend	101243
CD16/32 #	BV510	93	BioLegend	101333
CD27 *#	PE	LG.3A10	BD Biosciences	558754
CD27 *#	PE-Dazzle 594	LG.3A10	BioLegend	124228
CD27 #	FITC	LG.3A10	home made	n/a
CD31 #	PE	390	BioLegend	102408
CD34 #	AF700	RAM34	eBioscience	56-0341-82
CD45 #	BV605	30-F11	BioLegend	103139
CD45.1 #	BV650	A20	BioLegend	110735
c-Fms/ CD115 *	APC	AFS98	BioLegend	135510
c-Fms/ CD115 *#	BV711	AFS98	BioLegend	135515
c-Kit/ CD117 *#	PE-Cy7	2B8	eBioscience	25-1171-82
IL7Rα/ CD127 #	BV650	A7R34	BioLegend	135043
Flt3/ CD135 #	PE	A2F10	BD Biosciences	121351
B220 *#	FITC	RA3-6B2	BioLegend	103206
B220 *#	Percp-cy5.5	RA3-6B2	BioLegend	103236
B220 #	PB	RA3-6B2	BD Biosciences	558108
CCR2 #	PE	SA203G11	BioLegend	150610
CCL2 #	APC	2H5	BioLegend	505910
F4/80 #	APC-efluor780	BM8	eBioscience	47-4801-82
F4/80 #	AF700	BM8	eBioscience	56-4801-82
MHCII/ I-A/I-E #	AF700	M5/114.15.2	BioLegend	107622
MHCII/ I-A/I-E #	PE/Dazzle 594	M5/114.15.2	BioLegend	107648
MHCII/ I-A/I-E #	FITC	2G9	BD Biosciences	553623
MHCII/ I-A/I-E #	PB	M5/114.15.2	BioLegend	107620
RANK #	PE	R12-31	eBioscience	12-6612-82
Sca-1/ Ly-6A/E #	Percp-cy5.5	D7	eBioscience	45-5981-82
TLR5 *#	AF405	85B152.5	NOVUSBIO	NBP1-97728AF405
DAPI		N/A	Sigma	MBD0015
PI		N/A	BioLegend	421301
7-AAD		N/A	BioLegend	420403
LIVE/DEAD™ Fixable Near-IR Dead Cell Stain Kit #		N/A	Invitrogen	L34976

Antibodies used only for progenitor sorting are marked with *, antibodies only used for cell phenotyping are marked with # and antibodies used for both purposes are marked with *#.